Bulletin of Mathematical Biology, Vol. 59, No. 3, pp. 533–549, 1997
Elsevier Science Inc.

0092-8240/97 $17.00 + 0.00

S0092-8240(96)00106-1

PATTERN FORMATION IN SYSTEMS WITH ONE SPATIALLY DISTRIBUTED SPECIES

■ BARD ERMENTROUT
Department of Mathematics,
University of Pittsburgh,
Pittsburgh, PA 15260, U.S.A.

(*E.mail*: *bard@popeye.math.pitt.edu*)

■ MARK LEWIS
Department of Mathematics,
University of Utah,
Salt Lake City, UT 84112, U.S.A.

(*E.mail*: *mlewis@math.utah.edu*)

We describe a three-species mechanism for spatial pattern formation in which only one species spatially moves. We show that a bifurcation to traveling or standing waves occurs. We contrast this mechanism for pattern formation with the better known cases where more than one species moves. © 1997 Society for Mathematical Biology

1. Introduction. Pattern formation via the Turing instability has been the subject of numerous papers, and is particularly well characterized in two-species systems (see, e.g. Edelstein-Keshet, 1988 or Murray, 1989). In two-species models, the mechanism for the destabilization of the spatially uniform state requires spatial interactions between both species. In a typical scenario, there is an "activator" and an "inhibitor," and the inhibitor has longer range interactions than the activator. This results in so-called "lateral inhibition," and has been proposed as the mechanism for spatial patterning in dozens of systems. In two-species models, with lateral inhibition, the patterns that arise from the loss of stability are generally stationary, that is, they are time independent. It is well known (see, e.g. Ermentrout, 1981) that at least three species are required in order to get the appearance of spatio–temporal oscillations from a homogeneous rest state in systems of reaction–diffusion equations. In other systems, such as neural nets, bifurcation to traveling-wave trains or standing waves is possible for two-component systems, but only under rather unrealistic conditions (see Ermentrout, 1979).

Many biological systems involve situations in which only one of the species or components migrates. For example, in models of nerve conduction, only the membrane potential spatially interacts; the recovery and other variables interact only through the membrane potential. Models of a piece of cortex where there are local interneuronal interactions coupled with long-distance pyramidal cell models also involve "migration" of one species. Many plant–herbivore systems satisfy a similar constraint when there is only a single grazing species. Several reaction–diffusion systems obey this rule; for example, the model for cAMP excitability has only the extracellular cAMP moving and the cells and intracellular cAMP remaining bound (Tyson, 1989). Epidemiological models where only the uninfected are mobile provide another example.

We wish to explore the potential for bifurcating patterns arising from systems of this type. In particular, we will explore bifurcation to spatial and temporal waves that are driven by movement of a single species. The notion that systems where only one species migrates can lead to spontaneous symmetry breaking is counter to one's usual intuition about pattern formation. Thus, one of our goals is to show that once more than two components are involved, the "general principles" of pattern formation are not very useful. Since only one species is spatially distributed, it alone determines the scale of the pattern. In an infinite domain, changes in the space constant or diffusion coefficient cannot influence stability, only the scale of the pattern. This contrasts to pattern formation due to different spatial scales for the different species where stability depends crucially on the ratio of these scales.

In Section 2 of this paper, we show that in two-species systems, where only one species migrates, there can be no finite band of unstable wavenumbers. We then turn to three-species systems, and show that instabilities are possible and that they always result in bifurcation to spatially *and* temporally periodic patterns. That is, the loss of stability is through a Turing–Hopf bifurcation. Section 3 contains several examples involving both reaction–diffusion models and integro–differential equation models that arise from neural nets. We explore these numerically, and in the case of a spatially discrete model, give a complete bifurcation diagram.

2. Analysis of the Linearized System. Our strategy is to start with the linearized system, and then to analyze the spectrum as the wavenumber varies. We treat this rather abstractly in order to apply the results to any type of homogeneous "diffusion-like" spatial interaction. We assume that only one species can migrate, and that the spatial interaction is homogeneous and symmetric.

Let L denote the linearized spatial interaction. For example, in reaction–diffusion models,

$$Lu = \partial^2 u / \partial x^2 \tag{2.1}$$

while for neural network models,

$$Lu = \int_\Omega w(x, x')u(x')\,dx'. \tag{2.2}$$

Let ν_k denote the eigenvalues of L, i.e.

$$L\phi_k = \nu_k \phi_k. \tag{2.3}$$

In order that the pattern formation is not "built in" to the models, we assume that $\phi_0 = 1$ and that $\nu_0 > \nu_k$ for all k. That is, the fastest growing mode of the spatial interaction function is the spatially homogeneoous mode. Thus, we are not incorporating intrinsic pattern formation capability into the spatial interactions. We also assume boundary conditions on a finite domain of length l that permit us to order the discrete eigenvalues, $\nu_0 > \nu_1 > \cdots$. For example, if L is the diffusion operator with Neumann boundary conditions, the eigenvalues are $\nu_k = -D\pi^2 k^2/l^2$, where $k = 0, 1, 2, \ldots$. For a Gaussian convolution kernel on a periodic domain, the eigenvalues are $e^{-\sigma^2\pi^2k^2/l^2}$, where σ is the space constant of the interaction. We do not allow "Mexican hat" interactions where the maximal eigenvalue occurs at a nonzero wavenumber k.

Without loss in generality, we assume that the first component is the only one that spatially interacts. The general equations are then

$$\frac{du_1}{dt} = F_1(L[u_1](x), u_1, \ldots, u_n) \tag{2.4}$$

$$\frac{du_j}{dt} = F_j(u_1, \ldots, u_n), \qquad j \neq 1 \tag{2.5}$$

where F_1 is a monotone increasing function of the operator L. Since L is a homogeneous spatial operator, that is, it takes constant functions to constant functions, the fixed points of the spatially homogeneous system are also fixed points for the spatially varying system (2.4), (2.5.) The linearization about a fixed point has the simple form

$$\frac{dv_1}{dt} = cL[u_1](x) + \sum_{i=1}^{n} a_{i1}v_i, \qquad c > 0 \tag{2.6}$$

$$\frac{dv_j}{dt} = \sum_{j=1}^{n} a_{ij}v_i, \qquad j \neq 1. \tag{2.7}$$

The general solutions to this are of the form $v_j(x,t) = \xi_j \phi_k(x) e^{\lambda t}$ where λ are eigenvalues and ξ_j are components of the corresponding eigenvectors of the matrix

$$M(k) = \begin{pmatrix} a_{11} + c\nu_k & a_{21} & \cdots & a_{n1} \\ a_{12} & a_{22} & \cdots & a_{n2} \\ \vdots & \vdots & \vdots & \vdots \\ a_{1n} & a_{2n} & \cdots & a_{nn} \end{pmatrix}. \tag{2.8}$$

Before continuing, we can make some simplifying assumptions. We can absorb $c > 0$ into ν_k. We also replace ν_k by $\nu_k - \nu_0 + \nu_0$ and absorb ν_0 into a_{11}. We let $q_k = -(\nu_k - \nu_0)$ so that $q_0 = 0$ and $q_k > 0$ for $k > 0$. For example, in the case of the Gaussian convolution problem above, $q_k = 1 - e^{-\sigma^2 k^2 \pi^2 / l^2}$, and for the diffusion operator, $q_k = D\pi^2 k^2 / l^2$. Thus, we can rewrite $M(k)$ as

$$M(k) = \begin{pmatrix} a_{11} - q_k & a_{21} & \cdots & a_{n1} \\ a_{12} & a_{22} & \cdots & a_{n2} \\ \vdots & \vdots & \vdots & \vdots \\ a_{1n} & a_{2n} & \cdots & a_{nn} \end{pmatrix}. \tag{2.9}$$

The necessary conditions for pattern formation are that: (1) the eigenvalue with maximal real part for the matrix $M(k)$ must be negative for $k = 0$ and for k large, and (2) there must be an interval of values of k not containing 0 for which there are eigenvalues with positive real parts. This is the mechanism for the Turing instability. We make this more precise below.

The following lemma is a consequence of the properties of the determinant function.

LEMMA 1. *The characteristic polynomial of* $\mathrm{M(k)}$, $\sum_{j=0}^{n} c_j \lambda^j$, *has coefficients of the form*

$$c_j = \alpha_j + \beta_j q_k \tag{2.10}$$

where α_j, β_j *are constants.*

To precisely define spatially driven instabilities, we must assume that our system (2.9) depends on some parameter, say γ. We make the following definition.

Definition 1. The system (2.4) (2.5) undergoes a *spatially driven instability* if there is a unique eigenvalue (or conjugate pair) satisfying the characteris-

tic polynomial of $M(k)$ (2.9) with maximal real part $\lambda(q_k, \gamma) = r(q_k, \gamma) + i\omega(q_k, \gamma)$ such that

(a) $r(q_{k_0}, \gamma_0) = 0$, for some $q_{k_0} \neq 0$;
(b) $r(q_k, \gamma_0) < 0$, for all $|q_k| \neq |q_{k_0}|$;
(c) $\partial r(q_{k_0}, \gamma)/\partial\gamma|_{\gamma=\gamma_0} \neq 0$.

Remark. An illustration of spatially driven instabilities for the diffusion operator is shown in Fig. 1. If $\omega(q_{k_0}, \gamma_0) = 0$, then we call the spatial instability a Turing instability. This may lead to spatially inhomogeneous time-independent steady states, and is the mechanism for a large number of pattern-forming systems. If $\omega \neq 0$, then traveling or standing waves arise through a spatial Hopf (Turing–Hopf) bifurcation and lead to spatially and temporally periodic behavior.

Lemma 1 has two important consequences.

PROPOSITION 1. *The Turing instability cannot occur in systems of the form* (2.4), (2.5).

Proof. In order for the Turing instability to occur, there must be a zero eigenvalue so that the constant coefficient of the characteristic equation must vanish for some value $k_0 > 0$ and must be of the same sign for all other values of k. Since the coefficients are linear functions of q_k, this is impossible unless $k = 0$, which corresponds to homogeneous patterns.

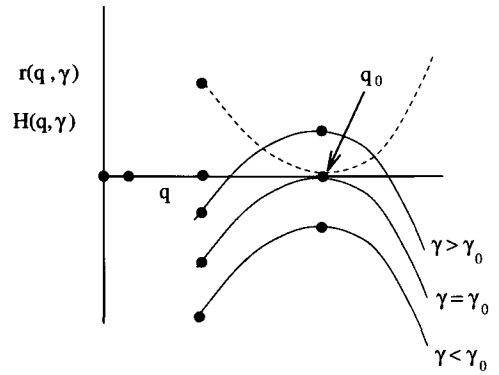

Figure 1. Spatial instability for the diffusion operator. The behavior of the real part of the maximal eigenvalue is given as a function of the spatial eigenvalue q and the bifurcation parameter γ. Although r is shown as a continuous function of q, for any given problem, the values of q_k are discrete. For $\gamma < \gamma_0$, all $r(q_k, \gamma) < 0$; for $\gamma = \gamma_0$, the real part vanishes at exactly one spatial eigenvalue q_{k_0}; for $\gamma > \gamma_0$, there is a band of q that yields instability ($r(q, \gamma) > 0$). Here, the domain length l was chosen so that $q_{k_0} = D\pi^2 k_0^2/l^2$ corresponds to the critical point for r. In general, this is not the case, as discussed below in the context of inducing pattern formation by changing the scale of spatial interactions on a finite domain. The dashed line shows the function H (2.11) derived from the Routh–Hurwitz conditions.

PROPOSITION 2. *No spatially driven instability can occur in systems of two or fewer species in which only one species spatially interacts.*

Proof. We have already established that loss of stability cannot occur at a zero eigenvalue. Thus, only Turing–Hopf instabilities are allowed. These do not happen in one-variable systems, and thus we consider only two-variable models. The Turing–Hopf bifurcation can only occur when the trace vanishes; our definition then requires that the trace have a local maximum at a non-zero value of k. The trace is

$$a_{11} + a_{22} + q_k.$$

If this vanishes at $k = k_0 > 0$, then it must be of opposite signs for k on either side of k_0, which means that there are other modes that have eigenvalues with positive real parts.

The two propositions imply that the "simplest" spatial bifurcation that can occur when only one species is mobile is the three-species Turing-Hopf bifurcation. A necessary condition for this is easily obtained from the Routh–Hurwitz criterion (see Edelstein-Keshet, 1988, p. 234). An imaginary eigenvalue occurs if c_2, c_1, c_0 are all positive and $H \equiv c_1 c_2 - c_0 = 0$. This leads to the following proposition.

PROPOSITION 3. *The following are necessary conditions for spatial instability to occur in a three-species model where only one species spatially interacts*:

(a) $\alpha_j > 0$ *and* $\alpha_1 \alpha_2 - \alpha_0 > 0$;
(b) $\beta_j > 0$;
(c) $\beta_1 \alpha_2 + \alpha_1 \beta_2 - \beta_0 < 0$.

Condition (b) is actually a little stronger than necessary; we require that $\alpha_j + \beta_j q_k > 0$ for all k. However, (a), (b) and $q_k \geqslant 0$ for all k ensure that this requirement is met.

Proof. The first condition just says that when $k = 0$, the eigenvalues have negative real parts. Condition (b) is required so that large wavenumbers remain stable and eliminates the "infinite wave number instability." To obtain condition (c), note that the Routh–Hurwitz criterion states that $H > 0$ for stability. We want this to vanish at a non-zero value of k and to be positive for all other values of k. Expanding H, we get

$$H = \alpha_1 \alpha_2 - \alpha_0 + (\beta_1 \alpha_2 + \alpha_1 \beta_2 - \beta_0) q_k + \beta_1 \beta_2 q_k^2. \tag{2.11}$$

Since $q_k \geqslant 0$, in order to get a local minimum, we must have the coefficient of q_k negative. This is condition (c).

Thus, if there is spatial interaction with only one variable, pattern formation, if it occurs at all, will always arise at a Turing–Hopf bifurcation since zero eigenvalues have been eliminated. A simple calculation shows that the frequency at the bifurcation is

$$\omega_0 = \sqrt{\alpha_1 + \beta_1 q_{k_0}}\,. \tag{2.12}$$

There are several interacting points about the spatial patterns. If we consider the case on the real line, then the spatial interaction length can be scaled out by redefining the spatial variable. This is because there is only *one* spatial scale in the problem. Although the now continuous spectrum for the spatial operator means that details of the bifurcation theory do not apply, changing the spatial scale should only affect the wavelength of the resulting pattern, not whether the pattern forms or the frequency of the oscillations. The limit as the spatial interactions become more localized is interesting since patterns become increasingly finer grained as the wavenumber increases, but when there are no spatial interactions, there is no pattern formation at all. For example, the diffusion operator with fixed q so that $r(q,\gamma) > 0$ yields patterns with a wavelength $2\pi\sqrt{D/q} \to 0$ as $D \to 0$, but $D = 0$ ensures no spatial patterns. The limit of $D = 0$ is singular since there is no longer any spatial coupling. Since space can be scaled arbitrarily, the amplitude and other properties of the solutions are the same no matter what D is as long as it is positive. In the usual two-species Turing mechanism, scaling both diffusion coefficients will behave in the same manner as this. However, scaling only one species' diffusibility will have different effects depending on which species is scaled. Reducing the spatial extent of the "inhibitor" leads to no pattern formation. Reducing the extent of the "activator" results in finer grains, but the amplitudes of the solutions get large, and as the diffusion of the "activator" tends to zero, the solutions become discontinuous.

On finite domains, with discrete values of k and corresponding discrete values of q_k, it is possible to first fix $\gamma > \gamma_0$ so that $r(q,\gamma) > 0$ for some open interval of q, and to then induce pattern formation by changing the scale of the spatial interactions relative to the domain length. For example, when D/l^2 is large, then possibly each of $q_k = D\pi^2 k^2/l^2$ for $k = 0, 1, 2, \ldots$ yields $r(q,\gamma) < 0$. This would simply mean that none of the eigenvalues for the spatial operator q_k fell in the interval where the growth rate $r(q,\gamma)$ was positive (Fig. 1). However, as D decreases, there may be a value of q_k that gives a spatial instability. For example, if $r(q,\gamma) > 0$ on the interval $0.1 < q < 0.2$, then D/l^2 would have to be at least as small as $0.2/\pi^2$ before there could be an value of q_k for which there was instability. This contrasts with the situation in the previous paragraph where q took on

continuous values. In the next section, we will also illustrate this point with a finite-dimensional system of discretely coupled cells in a ring.

We now derive conditions on the coefficients of the community matrix $A \equiv M|_{q_k=0}$ which will lead to the above type of Turing–Hopf instability. In the next section, we use these conditions applied to biological models. Let $A_{12}, A_{13}\, A_{23}$ denote the 2×2 matrices formed from A by eliminating, respectively, the third, second, and first row and column. The Routh–Hurwitz stability criteria are

$$q_k - \operatorname{tr} A > 0 \tag{2.13}$$

$$-\det A + q_k \det A_{23} > 0 \tag{2.14}$$

$$\det A + q_k \det A_{23}$$
$$+(q_k - \operatorname{tr} A)\big(\det A_{12} + \det A_{13} + \det A_{23} - q_k(a_{22}+a_{33})\big) > 0. \tag{2.15}$$

We require these to hold for $q_k = 0$ so that the system is stable to spatially homogeneous perturbations ($k = 0$). We also require that these hold for k large and positive so that there is no infinite wavelength instability. For the diffusion operator k large and positive, it means $q_k \to \infty$, and for the Gaussian convolution operator, it means $q_k \to 1$. In any case, we require $\det A_{23} > 0$ and $a_{22} - a_{23} < 0$. Now, consider where (2.13) and (2.14) are met, but (2.15) is violated for some range of q_k which does not contain 0. The function

$$H(q_k) = -q_k^2(a_{22}+a_{33}) + \big[\operatorname{tr} A(a_{22}+a_{33}) + \det A_{12} + \det A_{13}\big]q_k$$
$$- \operatorname{tr} A(\det A_{12} + \det A_{13} + \det A_{23}) + \det A \tag{2.16}$$

is negative over this range of q_k. At criticality, that is, when we are in the situation illustrated by Fig. 1, we have that

$$H(q_{k_0}) = 0$$
$$H'(q_{k_0}) = 0.$$

This yields the pure imaginary eigenvalues given by (2.12) which, in terms of the original matrix A, is

$$\omega_0 = \big\{\det A_{12} + \det A_{13} + \det A_{23} - q_{k_0}(a_{22}+a_{33})\big\}^{\frac{1}{2}}. \tag{2.17}$$

Note first that $0 = H'(q_{k_0})$ implies that

$$q_{k_0} = \frac{\operatorname{tr} A(a_{22} + a_{33}) + \det A_{12} + \det A_{13}}{2(a_{22} + a_{33})} \tag{2.18}$$

which, when substituted into $H(q_{k_0}) = 0$, yields

$$\begin{aligned}&\left[\operatorname{tr} A(a_{22} + a_{33}) + \det A_{12} + \det A_{13}\right]^2 \\ &\quad = 4(a_{22} + a_{33})\left[\operatorname{tr} A(\det A_{12} + \det A_{13} + \det A_{23}) - \det A\right]. \end{aligned} \tag{2.19}$$

Note that since $\operatorname{tr} A < 0$ and that $a_{22} + a_{33} < 0$, this means that in order for q_{k_0} to be positive, it is necessary for $\det A_{12} + \det A_{13}$ to be negative (see (2.18)). Furthermore, from (2.19), A_{23} must be larger in magnitude than $A_{12} + A_{13}$, which is negative.

3. Examples.

3.1. *Lotka–Volterra dynamics.* The first example we consider is an ecological model whose interactions are shown in Fig. 2(A). Assuming

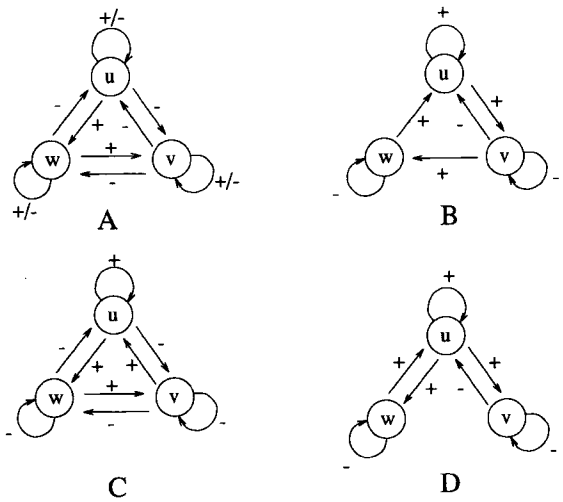

Figure 2. Interactions among three species that can give rise to pattern formation when only u spatially interacts. (A) An ecological model where u and v compete, w eats u and v eats w. This example is analysed in detail in the text. (B) A disease model with mobile susceptibles u, infecteds v and recovereds w. (C) A non-transitive predator prey model u eats v, v eats w and w eats u. (D) A neural model in which there is one principle neuron u which can synapse others like it, and a local inhibitory interneuron v and a local excitatory interneuron w. This example is described in detail in the text.

Lotka–Volterra dynamics with only u diffusing, we obtain

$$\frac{\partial u}{\partial t} = D\frac{\partial^2 u}{\partial x^2} + u(r_1 + a_{11}u + a_{12}v + a_{13}w) \tag{3.1}$$

$$\frac{\partial v}{\partial t} = v(r_2 + a_{21}u + a_{22}v + a_{23}w) \tag{3.2}$$

$$\frac{\partial w}{\partial t} = w(r_3 + a_{31}u + a_{32}v + a_{33}w). \tag{3.3}$$

The coexistence equilibrium satisfies

$$\begin{bmatrix} a_{11} & a_{12} & a_{13} \\ a_{21} & a_{22} & a_{23} \\ a_{31} & a_{32} & a_{33} \end{bmatrix} \begin{bmatrix} u_0 \\ v_0 \\ w_0 \end{bmatrix} = -\begin{bmatrix} r_1 \\ r_2 \\ r_3 \end{bmatrix}. \tag{3.4}$$

The linearized community matrix is

$$A = \begin{bmatrix} a_{11}u_0 & a_{12}u_0 & a_{13}u_0 \\ a_{21}v_0 & a_{22}v_0 & a_{23}v_0 \\ a_{31}w_0 & a_{32}w_0 & a_{33}w_0 \end{bmatrix}. \tag{3.5}$$

We choose $u_0 = v_0 = w_0 = 1$, the bifurcation parameter as $\gamma = a_{12}$ and

$$A = \begin{bmatrix} 0 & a_{12} & -1 \\ -8 & 0 & 8 \\ 1 & -2 & -2 \end{bmatrix}. \tag{3.6}$$

Thus, $r_1 = 1 - a_{12}$, $r_2 = 0$ and $r_3 = 3$. Using the results of the previous section, we find that $a_{12_0} = -1.494$, and the equation $Dk_0^2/l^2 = 1.738 \equiv q_0$ yields the critical wavenumber. The frequency of the bifurcation solution is $\omega_0 = 2.9192$. Fig. 3 shows the numerical solution for $a_{12} = 1.6 > a_{12_0}$ on an interval of length 10 with $D = 0.1$ and $D = 0.4$ and Neumann boundary conditions. Note that increasing the diffusion fourfold doubles the wavelength as expected.

To get some insight into the global pattern formation picture, we consider the same system coupled with discrete diffusion between two subpopulations u_1 and u_2. In this case, q_k takes on the two values, $q_0 = 0$ and $q_1 = 2D$. Unlike the continuous case, there are only two eigenmodes, the symmetric one and the anti-symmetric mode corresponding to the wavenumbers $k = 0$ and $k = 1$, respectively. Thus, the spatial pattern can be induced by using D as a bifurcation parameter. Indeed, for each value of

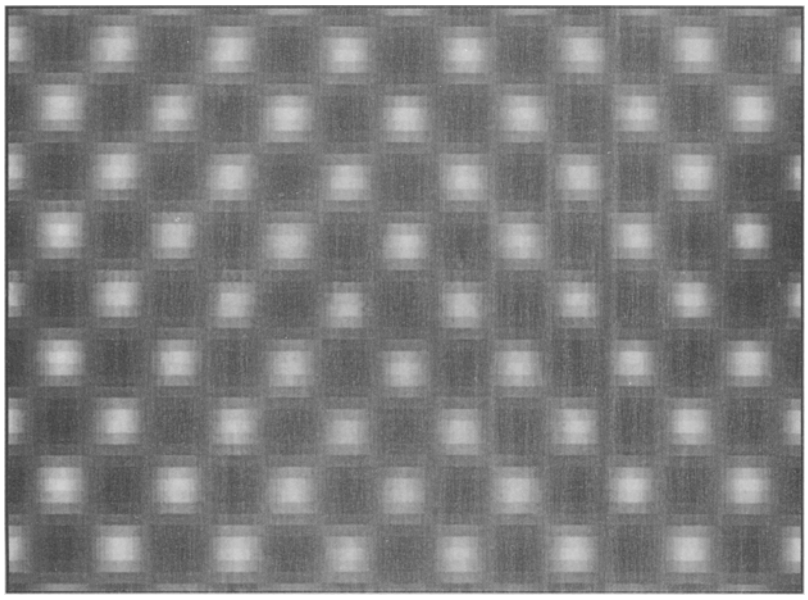

(A)

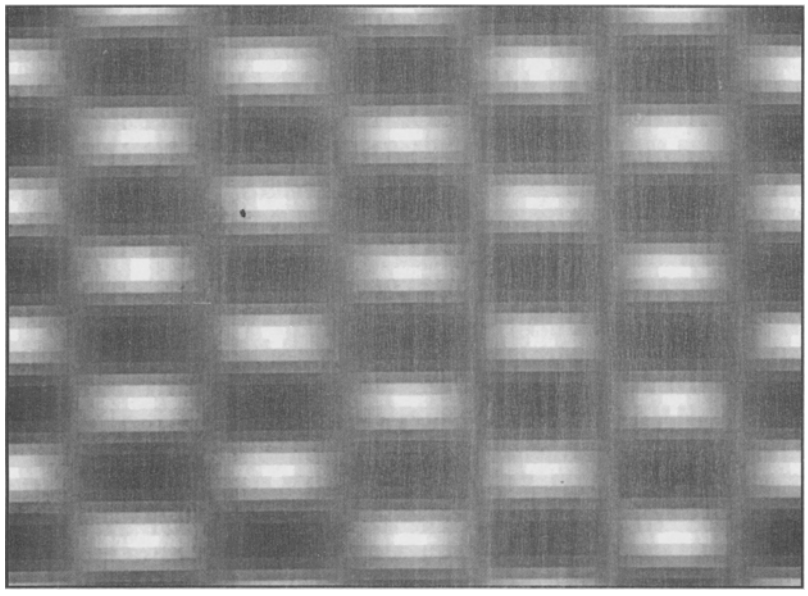

(B)

Figure 3. Space–time plots of the solutions to the ecological example given in Fig. 2(A). The variable $u(x,t)$ is plotted in grey scale with low ($u = 0.8$) population black and high ($u = 1.6$) populations white. Other species look identical up to a scale and a temporal phase shift. Time increases downward from 0 to 50 and space increases from left to right from 0 to 10. Upper picture: $D = 0.1$; lower picture $D = 0.4$. (Mesh is 200 points. Heun integration with a step size of 0.005 is used. Initial data are a small random perturbation from the rest state. Boundary conditions are Neumann.)

$a_{12} > a_{12_0}$, there will be two values of D where there is a Hopf bifurcation, $D_1(a_{12}) < D_2(a_{12})$ (Fig. 4 (A)). As $a_{12} \to a_{12_0}$, $D_j(a_{12} \to q_0/2 = 0.869$. For $D_1 < D < D_2$, there is a stable periodic solution in which $u_1(t)$ and $u_2(t)$ (as well as v, w) oscillate 180° out of phase. Fig. 4(B) illustrates the bifurcation diagram for $a_{12} = 1.6$ as D is varied, and Fig. 4(C) shows a solution to the coupled system when $\beta_1 = 1.6$ and $D = 1$.

Fig. 2(B) and (C) show some other interactions that can give rise to spontaneous spatio-temporal pattern formation. By way of example, linearized matrices yielding bifurcations for (B) and (C) with $q_{j_0} = 0.067$ and $q_{k_0} = 0.2$, respectively, are

$$A = \begin{bmatrix} 1.5 & -0.675 & 1 \\ 3 & -1 & 0 \\ 0 & 0.1 & -0.6 \end{bmatrix} \text{ and } A = \begin{bmatrix} 1.7 & 1 & -2 \\ -1 & -1 & 1 \\ 0.5 & -1 & -1 \end{bmatrix}. \tag{3.7}$$

Note that the structure of Fig. 2(B) is that of a classical epidemiological model with mobile susceptibles (u) and stationary infecteds (v) and recovereds (w). Recovereds are temporarily immune before entering the susceptible class. Here, arrows between u and v indicate infection via a nonlinear incidence function, and arrows from v to w and from w to u indicate movement generated by linear rate constants (Hethcote and Levin, 1989).

3.2. *A neural net.* In this example, we consider a neural network in which the coupling is not through diffusion, but rather through a convolution. The coupling constraints on this particular example are quite strong in order that no biological principles be violated. Fig. 2(D) shows the connections among the three cells. We imagine that u represents the activity of a cortical pyramidal cell, and that this cell sends synapses outward to other cells of the same type. Within the local area, we assume that there are two populations of interneurons: v is the activity of an inhibitory cell and w is that of the excitatory cell. We assume that the background or steady-state activity is set of 0. The equations are

$$\frac{\partial u}{\partial t} = f\left(a_{11}\int_0^L c(x,y)u(y,t)\,dy - a_{21}v + a_{31}w\right) \tag{3.8}$$

$$\frac{\partial v}{\partial t} = -a_{22}v + g(a_{12}u) \tag{3.9}$$

$$\frac{\partial w}{\partial t} = -a_{33}w + h(a_{13}u) \tag{3.10}$$

where f, g, h vanish at the origin and have a slope of 1 at that point. All coupling coefficients are positive. The connection function $c(x, y)$ is normalized so that its integral over y is 1 for all x.

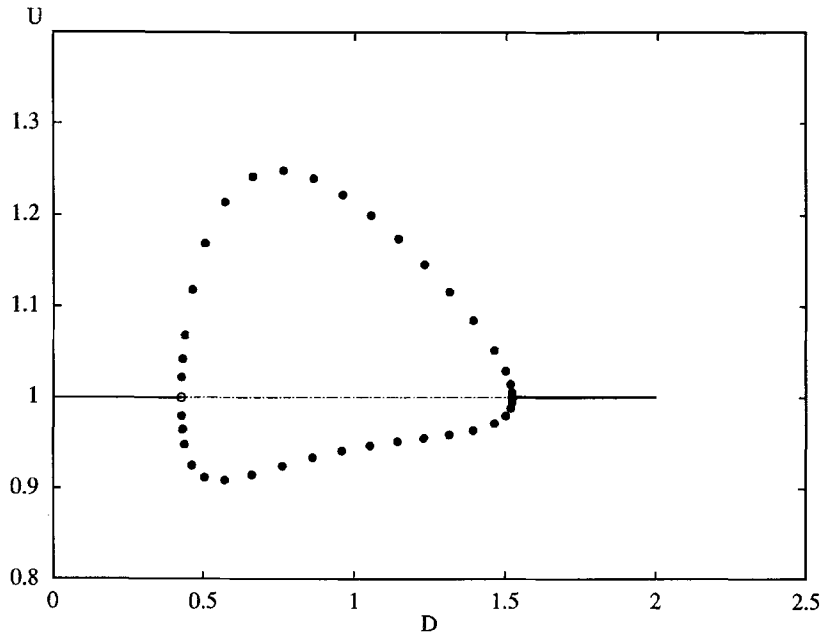

(A)

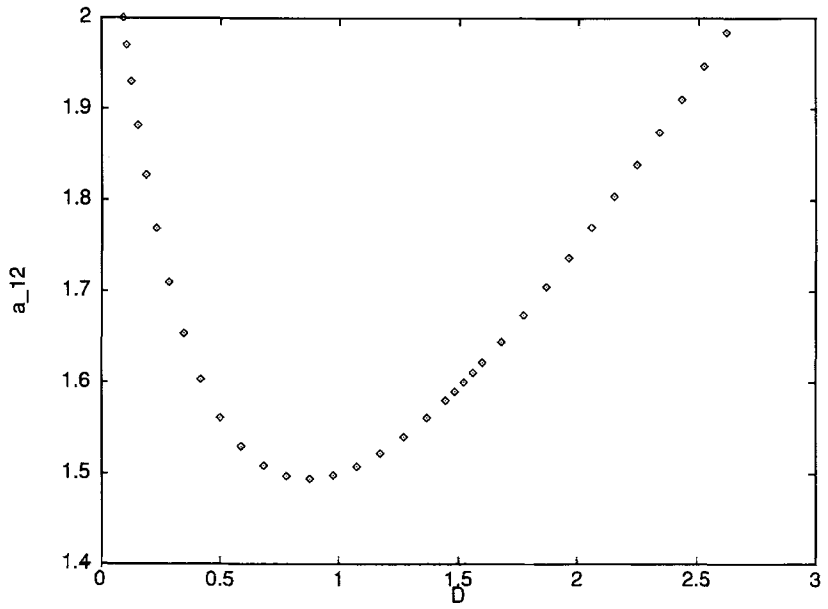

(B)

Figure 4. Global picture of pattern formation for the ecological example given in Fig. 2(A). (A) U as a function of the diffusion coefficient D for $a_{12} = 1.6$ showing the bifurcation to stable periodic solutions (filled circles) as D is varied. Stable fixed points are thick lines and unstable are thin. (B) Two-parameter curve of Hopf bifurcation points. Minimum is the critical value of a_{12} and D for pattern formation. For any a_{12} above this curve, the fixed point is unstable and there will be periodic solutions. (C) A periodic solution for $D = 1$ and $a_{12} = 1.6$ showing the two spatially distributed subpopulations of u, $u_1(t)$ and $u_2(t)$.

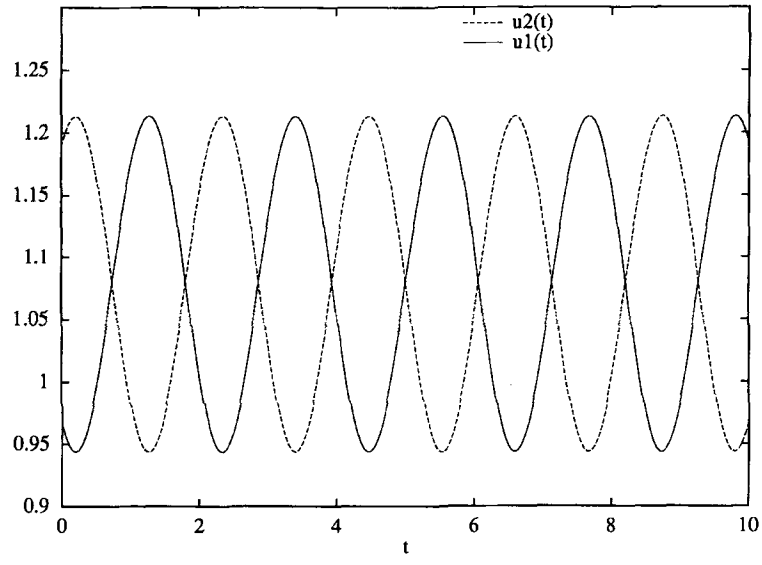

(C)

Figure 4. (*Continued*).

Note that this type of interaction matrix is found in nerve membrane models in which the three variables (u, v, w) represent, respectively, the membrane potential, a delayed rectifier, and an inward current (e.g. the Morris–Lecar model, 1981). In this case, the coupling would be via diffusion, and this would then represent a cable. Another example of this type of connection topology is found in a neural model due to Goldstein and Rall (1974).

For the present example, we take

$$f(u) = 4.046\left(\frac{1}{1+e^{-(u-.25)}} - \frac{1}{1+e^{.25}}\right) \tag{3.11}$$

which vanishes at 0 and has the required slope. For simplicity, we assume that $g(u) = h(u) = u$. With the value a_{21} as the bifurcation parameter, we set $a_{31} = 7.4$, $a_{11} = 9.5$, $a_{22} = 6$, $a_{33} = 3.3$, $a_{13} = 2$, $a_{12} = 7.875$. The connectivity is periodic over the length of the domain $L = 1$, and is given by $c(x, y) = Ke^{-|x-y|/\sigma}$ with $\sigma = 0.02$ and $K = 25$ chosen so the integral is 1. With this choice of parameters, we find that $a_{21_c} = 9.9638$ and $q_{k_0} = 0.045$. With the choice of the exponential kernel, we thus find that $k_0 \approx 0.04/\sigma$ and $\omega_0 \approx 3$. Fig. 5 shows a simulation with $a_{21} = 10$. The simulation shows that traveling waves have bifurcated from the trivial state and have a wavelength of 2. The wavelength is exactly what the linear analysis predicts,

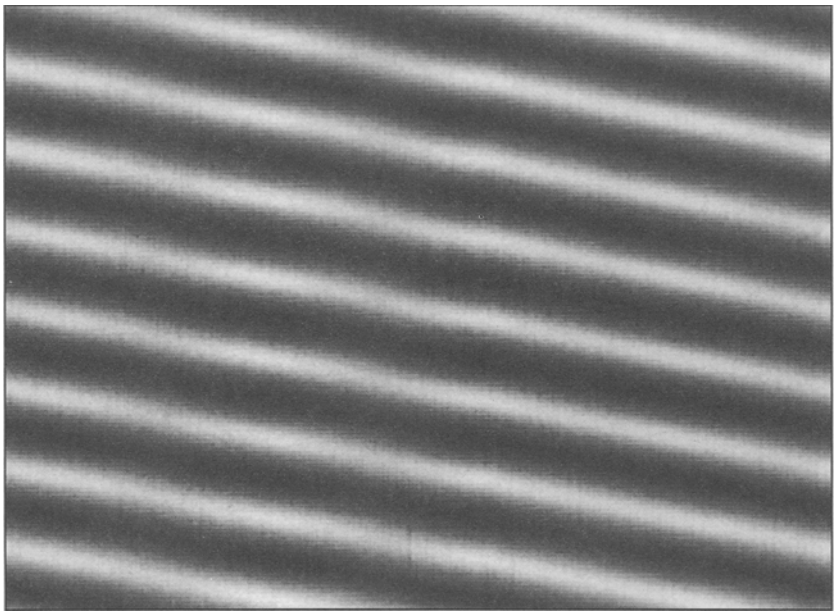

Figure 5. Numerical solution to (3.8, 3.11) on a periodic domain of length 1 with a discretization of 200 points. Heun's method is used with a step size of 0.025. Initial data are a small random perturbation from 0. Space is horizontal and time is vertical; time interval is $t = 30$–$t = 45$. Grey scale represents $u = -0.2$ (black) to $u = 0.4$ (white).

and since the length of time illustrated in the figure is 15 time units, the period of the oscillation is about 1.9, which gives a frequency that is slightly higher than that at the Hopf bifurcation.

4. Discussion. We have shown that spontaneous symmetry breaking patterns can occur in systems in which *only one* variable interacts spatially. All remaining variables are localized. The intuition behind this type of pattern formation is not clear; there are no simple statements such as "lateral inhibition" causes pattern formation. Here, there are a variety of different scenarios, and there seems to be little common about them. For example, in the community example, no variable exerts self positive feedback, while in the neural net example, this feedback is required for the instability. In two-species systems, the interactions necessary for pattern formation are simple; the cross terms are of the "negative" feedback type. In three-species models, the cross terms are of both types, and there seems to be no obvious pattern to them. In the two worked examples, the diffusing species had negative and positive feedback loops. We do not know if this is a necessary condition. However, in the neural net model, if both feedback loops to u are negative, there will be no pattern formation, nor will there be if both

are positive. Thus, this mechanism seems to require some fine balance between the interactions, and thus is not as robust as the typical two-species pattern-forming systems.

The notion that spatio–temporal bifurcations can occur in coupled systems is not new. Smale (1973) and Kishimoto *et al.* (1983) show that three- or four-species systems with diagonal (but not scalar) diffusion can exhibit spatially patterned oscillations. Ermentrout (1981) constructs examples in three-species systems. However, as in the Smale and Kishimoto *et al.* work, each species is allowed to diffuse. A two-component neural net in which spatial interactions were allowed for both components was also shown to exhibit Turing–Hopf bifurcations (Ermentrout, 1979). What is unusual in the present case is that there is only one spatial scale, so that the instability is driven by the *dynamics* rather than by the *differences in spatial scales*. Levin and Segel (1985) explore some scalar models (thus with only one mobile species) in which the spatial interactions are nonlinear; these nonlinearities lead to spatial patterning. Thus, the Turing mechanism is not the only way to get such patterns. Our main goal in this note was to provoke discussion about the current understanding of mechanisms for spontaneous pattern formation in biological systems.

The work of B. Ermentrout was supported in part by NSF Grant DMS-93-03706. The work of M. Lewis was supported in part by NSF Grant DMS-9457816 and a research fellowship from the Alfred P. Sloan Foundation.

REFERENCES

Edelstein-Kesher, L. 1988. *Mathematical Models in Biology*. New York: Random House.

Ermentrout, G. B. 1979. Symmetry breaking in stationary, homogeneous, isotropic neural nets. Ph.D. thesis, University of Chicago, Department of Biophysics and Theoretical Biology.

Ermentrout, G. B. 1981. Stable small amplitude solutions in reaction-diffusion systems. *Quart. Appl. Math.* 61–86.

Goldstein, S. S. and W. Rall. 1974. Changes in action potential shape and velocity for changing core conductor geometry. *Biophys. J.* **14**, 731–757.

Hethcote, H. W. and S. A. Levin. 1989. Periodicity in epidemiological models. In *Applied Mathematical Ecology*, L. Gross, T. G. Hallam and S. A. Levin (Eds). Berlin: Springer-Verlag.

Kishimoto, K., M. Mimura and K. Yoshida. 1983. Stable spatio-temporal oscillations of diffusive Lotka–Volterra system with three or more species. *J. Math. Biol.* **18**, 213–221.

Levin, S. A. and L. A. Segel. 1985. Pattern generation in space and aspect. *SIAM Rev.* **27**, 45–67.

Morris, C. and H. Lecar. 1981. Voltage oscillations in the barnacle giant muscle fiber. *Biophys. J.* **35**, 193–213.

Murray, J. D. 1989. *Mathematical Biology*. New York: Springer-Verlag.
Smale, S. 1974. A mathematical model of two cells via Turing's equation. In *Some Mathematical Questions in Biology. V*, J. D. Cowan (Ed). Providence, RI: American Mathematical Society.
Tyson, J. J. 1989. Cyclic-AMP waves in *Dictyostelium*: specific models and general theories. In *Cell to Cell Signalling: From Experiments to Theoretical Models*, A. Goldbeter (Ed), pp. 521–540. New York: Academic Press.

Received 21 May 1996
Revised version accepted 16 September 1996